Virology **288,** 212–222 (2001)
doi:10.1006/viro.2001.1098, available online at http://www.idealibrary.com on IDEAL®

# Further Identification and Characterization of Novel Intermediate and Mature Cleavage Products Released from the ORF 1b Region of the Avian Coronavirus Infectious Bronchitis Virus 1a/1b Polyprotein

H. Y. Xu, K. P. Lim, S. Shen, and D. X. Liu[1]

*Institute of Molecular Agrobiology, 1 Research Link, The National University of Singapore, Singapore 117604*

*Received February 13, 2001; returned to author for revision April 2, 2001; accepted July 19, 2001*

The coronavirus 3C-like proteinase is one of the viral proteinases responsible for processing of the 1a and 1a/1b polyproteins to multiple mature products. In cells infected with avian coronavirus infectious bronchitis virus (IBV), three proteins of 100, 39, and 35 kDa, respectively, were previously identified as mature cleavage products released from the 1b region of the 1a/1b polyprotein by the 3C-like proteinase. In this report, we show the identification of two more cleavage products of 68 and 58 kDa released from the same region of the polyprotein. In addition, two stable intermediate cleavage products with molecular masses of 160 and 132 kDa, respectively, were identified in IBV-infected cells. The 160-kDa protein was shown to be an intermediate cleavage product covering the 100- and 68-kDa proteins, and the 132-kDa protein to be an intermediate cleavage product covering the 58-, 39-, and 35-kDa proteins. Immunofluorescent staining of IBV-infected cells and cells expressing individual cleavage products showed that the 100-, 68-, and 58-kDa proteins were associated with the membranes of the endoplasmic reticulum, and the 39- and 35-kDa proteins displayed diffuse distribution patterns. 

## INTRODUCTION

Coronavirus gene expression involves the expression of six to seven mRNA species. In cells infected with the prototype species of the Coronaviridae, avian coronavirus infectious bronchitis virus (IBV), six mRNA species are detected. These include the genome-length mRNA (mRNA1) of 27.6 kilobases (kb) and five subgenomic mRNA species (mRNAs 2–6) with sizes ranging from 2 to 7 kb. The 5′-terminal unique region of mRNA 1 contains two large ORFs, 1a and 1b, encoding the 441-kDa 1a and 741-kDa 1a/1b polyproteins (Boursnell *et al.,* 1987) (Fig. 1). The two polyproteins are cleaved by two viral proteinases to produce functional products associated with viral replication (Ziebuhr *et al.,* 2000) (Fig. 1).

The first proteinase was identified to be included in a 195-kDa cleavage product, which contains a papain-like proteinase domain encoded by ORF 1a from nucleotides 4242 to 5553 (Lim *et al.,* 2000). This proteinase was shown to be involved in cleavage of the N-terminal region of the 1a and 1a/1b polyproteins at two G–G dipeptide bonds ($G^{673}$–$G^{674}$ and $G^{2265}$–$G^{2266}$) to release two mature products of 87 and 195 kDa (Liu *et al.,* 1995; Lim and Liu, 1998; Lim *et al.,* 2000). The second proteinase was identified as a 33-kDa protein in IBV-infected cells (Liu and Brown, 1995; Lim *et al.,* 2000; Ng and Liu, 2000). This serine proteinase belongs to the picornavirus 3C proteinase group (3C-like proteinase) and was shown to mediate cleavage of the 1a and 1a/1b polyproteins at more than 10 Q–S(G, N) dipeptide bonds to release mature cleavage products (Liu *et al.,* 1994, 1997, 1998; Ng and Liu, 1998, 2000).

In addition to the viral proteinases, understanding of the functions of other cleavage products from the 1a and 1a/1b polyproteins is emerging. For example, the 71-kDa protein released from the human coronavirus 1a/1b polyprotein was shown to possess ATPase and RNA duplex-unwinding activities, confirming the previous predication that the protein may be the viral helicase (Heusipp *et al.,* 1997a; Seybert *et al.,* 2000a,b). Immunofluorescence and biochemical studies demonstrated that several cleavage products are membrane-associated and colocalize with the viral RNA replication–transcription machinery (Bost *et al.,* 2000; Denison *et al.,* 1999; Ng and Liu, 2000; Schiller *et al.,* 1998; Shi *et al.,* 1999; Sims *et al.,* 2000; Ziebuhr and Siddell, 1999; van der Meer *et al.,* 1999), suggesting the involvement of these products in viral RNA replication. More recent studies showed that the first cleavage product of mouse hepatitis virus-A59 (MHV-A59) 1a and 1a/1b polyproteins, p28, might play a direct role in viral RNA synthesis together with polymerase and helicase (Bost *et al.,* 2000; Sims *et al.,* 2000). Other cleavage products, such as the MHV 22-kDa protein, may segregate into different but tightly associated membrane populations which may serve independent

[1] To whom reprint requests should be addressed. E-mail: liudx@ima.org.sg.

0042-6822/01 $35.00

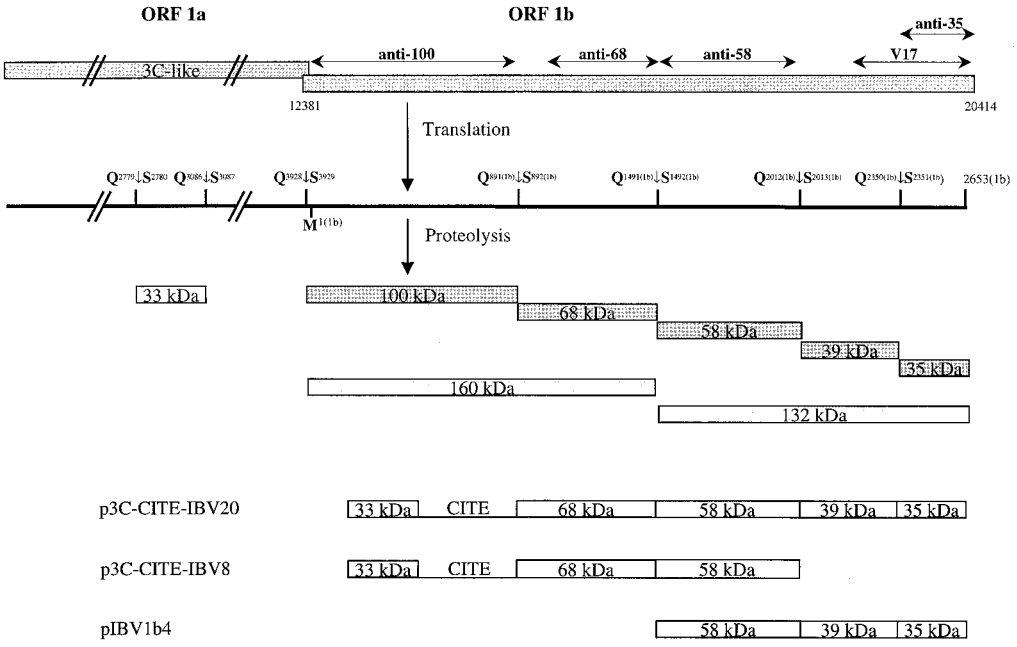


FIG. 1. Diagram showing the structure of ORF 1a and 1b and the proteolytic processing map of the 1b region of the 1a/1b polyprotein. The regions used to raise anti-100, anti-68, anti-58, anti-39, and V17 and the positions of the identified Q–S(G) cleavage sites of the 3C-like proteinase are shown. The first amino acid position ($M^{1(1b)}$) of the 1b region of the 1a/1b polyprotein was counted from the methionine residue encoded by nucleotides 12459 to 12461. Also shown are the positions of the 33-kDa 3C-like proteinase, the intermediate and mature cleavage products released from the 1b region, and the diagram of the two dicistronic constructs.

functions during viral replication (Bost *et al.,* 2000; Sims *et al.,* 2000).

In previous reports, we demonstrated that four previously predicted Q–S(G) dipeptide bonds located in the 1b region of the 1a/1b polyprotein are genuine cleavage sites of the 3C-like proteinase (Liu *et al.,* 1994, 1998; Liu and Brown, 1995). Taken together with the N-terminal cleavage site identified for releasing the 100-kDa protein, cleavage at these positions would result in the release of five mature products with molecular masses of approximately 100, 68, 58, 39, and 35 kDa, respectively (Fig. 1). Among them, the 100-, 39-, and 35-kDa proteins were specifically identified in IBV-infected cells. In this communication, we report the identification of the two previously unidentified products, the 68- and 58-kDa proteins, in IBV-infected cells with newly raised region-specific antisera. Meanwhile, two relatively stable intermediate cleavage products with molecular masses of approximately 160 and 132 kDa were identified. Analysis of the expression and processing kinetics showed that both the 160- and 132-kDa intermediate cleavage products coexist with their final cleavage products during the viral replication cycle. Furthermore, immunofluorescence analysis showed that the 100-, 68-, and 58-kDa proteins were associated with the membranes of the endoplasmic reticulum (ER), while the 39- and 35-kDa proteins displayed diffuse distribution patterns.

## RESULTS

### Further identification of novel intermediate and mature cleavage products encoded in the ORF1b region in IBV-infected cells

In our previous reports, four Q–S(G) dipeptide bonds, $Q^{891(1b)}$–$S^{892(1b)}$, $Q^{1492(1b)}$–$G^{1493(1b)}$, $Q^{2012(1b)}$–$S^{2013(1b)}$, and $Q^{2350(1b)}$–$S^{2351(1b)}$, located in the ORF 1b region and encoded by nucleotides 15129–15134, 16929–16934, 18492–18497, and 19506–19511, respectively, were demonstrated to be the cleavage sites of the 3C-like proteinase (Liu *et al.,* 1994, 1998) (Fig. 1). Taken together with the $Q^{3928}$–$S^{2929}$ dipeptide bond (encoded by nucleotides 12310–12315) identified as the N-terminal cleavage site of the 100-kDa protein, cleavage at these positions would result in the release of five mature products with molecular masses of approximately 100, 68, 58, 39, and 35 kDa. Among them, the 100-, 39-, and 35-kDa proteins were specifically identified in IBV-infected cells (Liu *et al.,* 1994, 1998). To further identify and characterize the cleavage products, four new region-specific antisera, anti-100, anti-68, anti-58, and anti-35, were raised in rabbits against bacterially expressed viral proteins. The IBV proteins used to raise these antisera were encoded by nucleotides 12447–15131, 15536–16787, 16932–18494, and 19509–20414, respectively (Fig. 1). Anti-100 was raised to replace V-58, which was raised against the IBV sequence encoded by nucleotides 14492–15520, and was used to identify the 100-kDa protein in IBV-

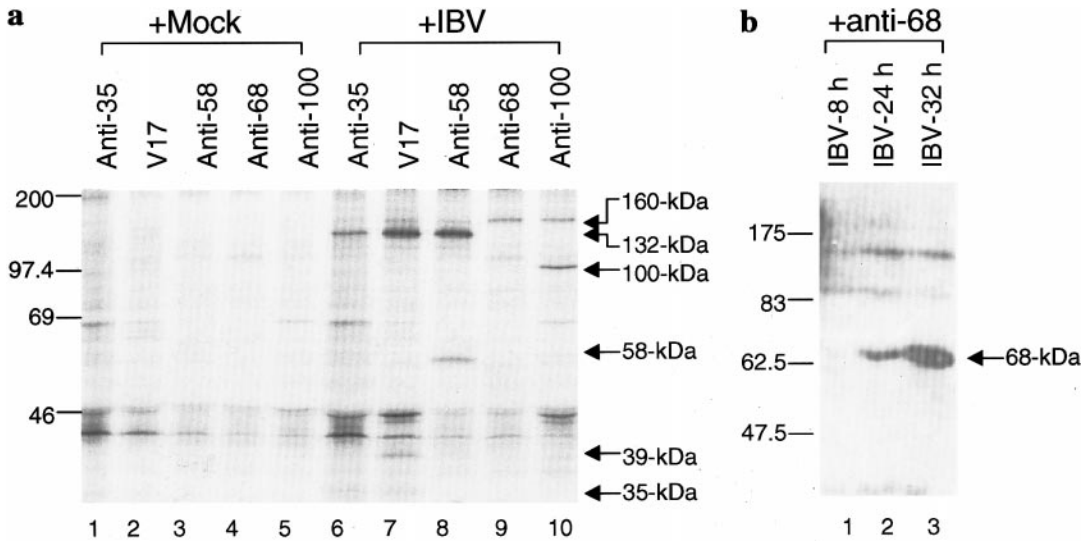


FIG. 2. (a) Immunoprecipitation analysis of the cleavage products released from the 1b region of the 1a/1b polyprotein in IBV-infected Vero cells. Confluent monolayers of Vero cells were infected with IBV at a m.o.i. of 3 PFU per cell. The IBV-infected (IBV) and mock-infected (Mock) cells were labeled with [$^{35}$S]methionine and cysteine, lysates were prepared, and polypeptides were immunoprecipitated with anti-100 (lanes 5 and 10), anti-68 (lanes 4 and 9), anti-58 (lanes 3 and 8), V17 (lanes 2 and 7), and anti-35 (lanes 1 and 6). The radiolabeled polypeptides were separated on an SDS–12.5% polyacrylamide gel and detected by fluorography. Numbers on the left indicate molecular mass in kilodaltons. (b) Western blotting analysis of the 68-kDa protein in IBV-infected Vero cells. Confluent monolayers of Vero cells were infected with IBV at a m.o.i. of 3 PFU per cell and were harvested at 8, 24, and 32 h postinfection, respectively. Polypeptides were separated on an SDS–12.5% polyacrylamide gel, transferred to a nitrocellulose membrane, and detected by Western blot with anti-68. Numbers on the left indicate molecular mass in kilodaltons.

infected cells (Liu *et al.,* 1994). The specificities of these antisera were tested by immunoprecipitation assay, showing that they could specifically precipitate their target proteins synthesized in both the *in vitro* system and intact cells (data not shown).

To identify the cleavage products in IBV-infected cells, confluent monolayers of Vero cells were infected with IBV at a m.o.i. of approximately 3 PFU per cell. To reduce the background, 5 $\mu$g/ml of actinomycin D was added to the culture medium at 2 h postinfection and cells were labeled with [$^{35}$S]methionine and cysteine at 6 h postinfection. Cell lysates were prepared from cells harvested at 8 h postinfection and subjected to immunoprecipitation with anti-100, anti-68, anti-58, V17, and anti-35. V17 was raised against the IBV polypeptides encoded by nucleotides 19154–20414 and used to detect the 39- and 35-kDa proteins in IBV-infected cells in a previous report (Liu *et al.,* 1998). Immunoprecipitation with anti-100 resulted in the detection of the 100-kDa protein and a protein with an apparent molecular mass of 160 kDa (Fig. 2a, lane 10). The 160-kDa protein was also detected by anti-68 (Fig. 2a, lane 9). No product corresponding to the 68-kDa putative helicase domain-containing protein was detected by anti-68 (Fig. 2a, lane 9). The detection of the 160-kDa protein with the two N-terminally specific antisera and the apparent molecular mass of the protein suggest that it may be an intermediate cleavage product containing the 100-kDa and the putative 68-kDa proteins. Immunoprecipitation of the same lysates with anti-58 resulted in the detection of two products with apparent molecular masses of 58 and 132 kDa (Fig. 2a, lane 8). The 132-kDa protein was also immunoprecipitated by V17 and anti-35 (Fig. 2a, lanes 6 and 7). In addition, V17 also precipitated specifically the 39- and 35-kDa proteins (Fig. 2a, lane 7). Once again, very weak immunoprecipitation of the 35-kDa protein was observed (Fig. 2a, lane 7). The 35-kDa protein was also weakly immunoprecipitated by anti-35 (Fig. 2a, lane 6). The detection of the 132-kDa protein by the three C-terminally specific antisera and the apparent molecular mass of the protein suggest that it may be an intermediate cleavage product derived from the C-terminal region of the polyprotein. Interestingly, the three C-terminally specific antisera also weakly immunoprecipitated the 160-kDa protein (Fig. 2a, lanes 6–8). The reason for this result is currently unclear, but it may reflect the interaction among the cleavage products.

As immunoprecipitation with anti-68 failed to detect the putative 68-kDa protein in IBV-infected Vero cells, we then tried to detect the protein by Western blot with the same antiserum. For this purpose, cell lysates were prepared from IBV-infected Vero cells harvested at 8, 24, and 32 h postinfection, respectively, and subjected to Western blotting analysis. As shown in Fig. 2b, a polypeptide with an apparent molecular mass of 68 kDa was specifically detected in lysates prepared from cells harvested at 24 h postinfection (lane 2), and the expression of the protein was dramatically increased at 32 h postinfection (lane 3).

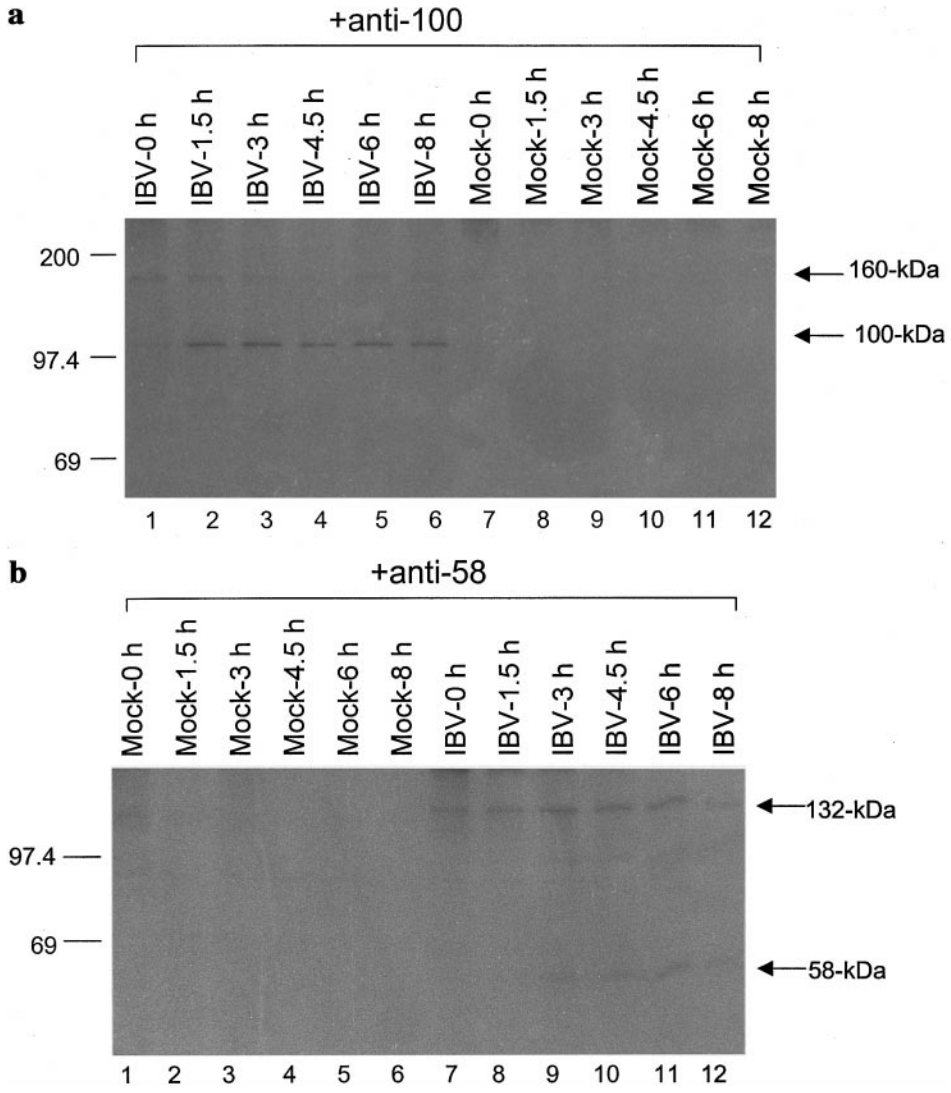


FIG. 3. (a) Pulse–chase analysis of the expression, processing, and accumulation of the 160- and 100-kDa products in IBV-infected Vero cells. Confluent monolayers of Vero cells were infected with IBV at a m.o.i. of 3 PFU per cell, labeled with [$^{35}$S]methionine and cysteine for 2 h at 6 h postinfection, and chased with a 10-fold excess of cold methionine. The cells were harvested after chase for 0, 1.5, 3, 4.5, 6, and 8 h, respectively. Cell lysates were prepared and immunoprecipitated with anti-100. The radiolabeled polypeptides were separated on an SDS–10% polyacrylamide gel and detected by fluorography. Numbers on the left indicate molecular mass in kilodaltons. (b) Pulse–chase analysis of the expression, processing, and accumulation of the 132- and 58-kDa products in IBV-infected Vero cells. The radiolabeled polypeptides were separated on an SDS–15% polyacrylamide gel.

### Expression and processing kinetics of the ORF 1b region of the 1a/1b polyprotein in IBV-infected Vero cells

As the 160- and 132-kDa proteins may represent stable intermediate cleavage products, time-course experiments were carried out to investigate the expression and processing kinetics of the two products in IBV-infected cells. For this purpose, confluent monolayers of Vero cells were infected with IBV at a m.o.i. of approximately 3 PFU per cell and were labeled for 2 h with [$^{35}$S]methionine at 6 h postinfection. The cells were then washed with complete medium and chased with a 10-fold excess of cold methionine until they were harvested at appropriate times. Immunoprecipitation of cell lysates with anti-100 showed the detection of both the 100- and 160-kDa proteins throughout the time course (Fig. 3a). The 100-kDa protein appeared at the beginning of the time course, peaked after chase for 1.5 h, and remained stable at the end of the time course (Fig. 3a, lane 2). The 160-kDa protein peaked at the beginning of the time course and remained detectable after chase for 7.5 h (Fig. 3a, lanes 1–6). Slight and gradual reduction of the 160-kDa protein over time was observed (Fig. 3a). These results demonstrate that the 160-kDa protein is a relatively stable intermediate cleavage product coexisting with the 100-kDa mature cleavage product during the IBV infection cycle.

Similarly, immunoprecipitation of cell lysates with anti-

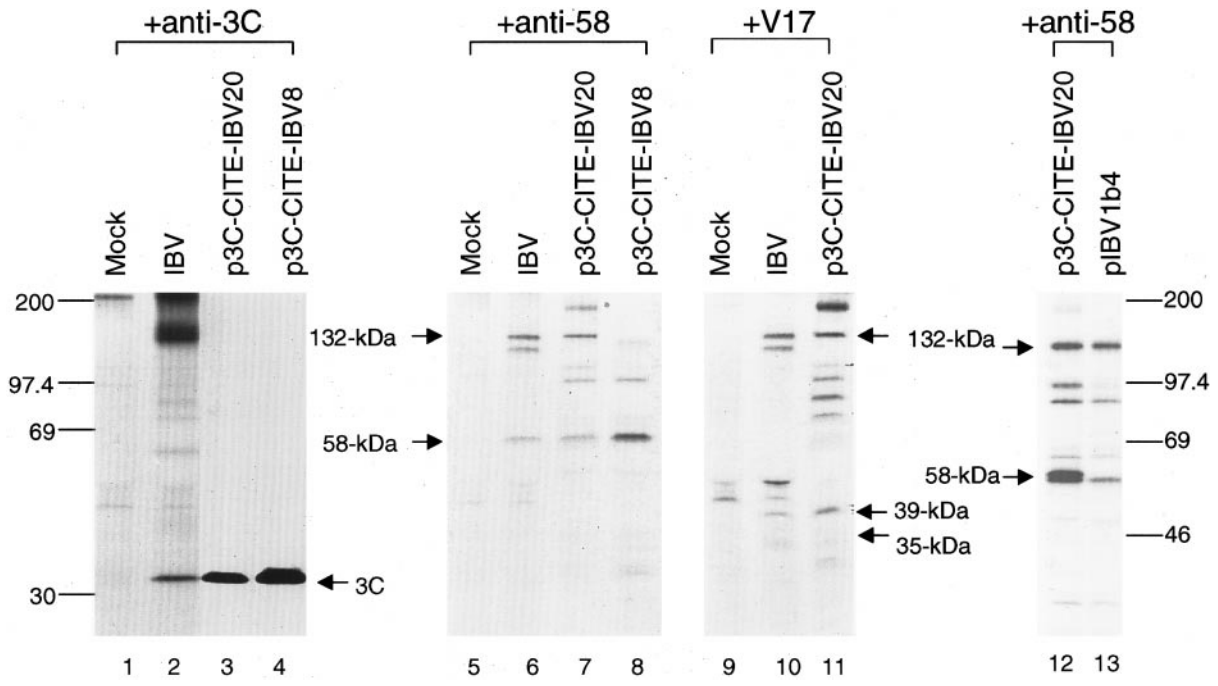


FIG. 4. Comparative analysis of the 132- and 58-kDa proteins expressed and processed in cells transfected with p3C-CITE-IBV20, p3C-CITE-IBV8, and pIBV1b4 and in IBV-infected cells. Plasmid DNAs were expressed in Cos-7 cells using the vaccinia virus-T7 expression system (Fuerst *et al.,* 1986). Semiconfluent monolayers of Cos-7 cells were infected with a recombinant vaccinia virus (vTF7-3), transfected with plasmid DNA using DOTAP according to the instructions of the manufacturer (Roche), and labeled with [$^{35}$S]methionine and cysteine, and lysates were prepared. Cell lysates prepared from mock-infected (lanes 1, 5, and 9) and IBV-infected (lanes 2, 6, and 10) Vero cells and transfected cells (lanes 3, 4, 7, 8, 11–13) were immunoprecipitated with anti-3C (lanes 1–4), anti-58 (lanes 5–8, 12, and 13), and V17 (lanes 9–11). The radiolabeled polypeptides were separated on an SDS–12.5% polyacrylamide gel and detected by fluorography. Numbers indicate molecular mass in kilodaltons.

58 showed the detection of both the 132- and 58-kDa proteins (Fig. 3b). The 132-kDa protein appeared at the beginning of the time course, peaked after chased for 3 h, and remained detectable at the end of the time course (Fig. 3b, lanes 9–12). The 58-kDa protein was first seen after chased for 3 h and gradually increased over time (Fig. 3b, lanes 9–12). Interestingly, a product with an apparent molecular mass of 97 kDa, representing an intermediate cleavage product containing the 58- and 39-kDa proteins (Liu *et al.,* 1998), was weakly detected and briefly observed during the time course (Fig. 3b, lanes 9 and 10), indicating that it is not a stable intermediate cleavage product. The coexistence of the 132- and 58-kDa proteins over time suggests that the 132-kDa protein is a stable intermediate cleavage product.

### Further characterization and definition of the coding sequences of products processed from the C-terminal 200-kDa region of the 1a/1b polyprotein

Two dicistronic constructs, p3C-CITE-IBV20 and p3C-CITE-IBV8, were made and expressed to characterize the expression and processing patterns of the C-terminal 200-kDa region of the 1a/1b polyprotein. In these two constructs, the region coding for the 3C-like proteinase was placed between the T7 promoter and the internal ribosome entry site (IRES) of encephomyolitis virus (EMCV), and the IBV sequences from nucleotides 15132–20506 and 15132–18495, respectively, were cloned downstream of IRES (Fig. 1).

Expression of both constructs in Cos-7 cells resulted in the detection of the 33-kDa 3C-like proteinase, which comigrates on SDS–PAGE with the 33-kDa protein detected in IBV-infected cells (Fig. 4, lanes 2–4). Immunoprecipitation of cell lysates prepared from p3C-CITE-IBV20-transfected cells with anti-58 led to the detection of three protein species with apparent molecular masses of 200, 132, and 58 kDa, respectively (Fig. 4, lane 7). The 200-kDa protein represents the full-length product encoded by the IBV 1b sequence present in this plasmid, and the 132- and 58-kDa proteins comigrated with the 132- and 58-kDa proteins detected in IBV-infected cells (Fig. 4, lanes 6 and 7). Immunoprecipitation of cell lysates prepared from p3C-CITE-IBV8-transfected cells with anti-58 led to the detection of the 58-kDa protein and a product with an apparent molecular mass of 125 kDa (Fig. 4, lane 8). The 125-kDa protein may represent the full-length product encoded by the 1b sequence present in this construct. Immunoprecipitation of cell lysates prepared from p3C-CITE-IBV20-transfected cells with antiserum V17 led to the detection of the 200-, 132-, 39-, and 35-kDa proteins (Fig. 4, lane 11). The 132-, 39-, and 35-kDa proteins comigrated with the three equivalent

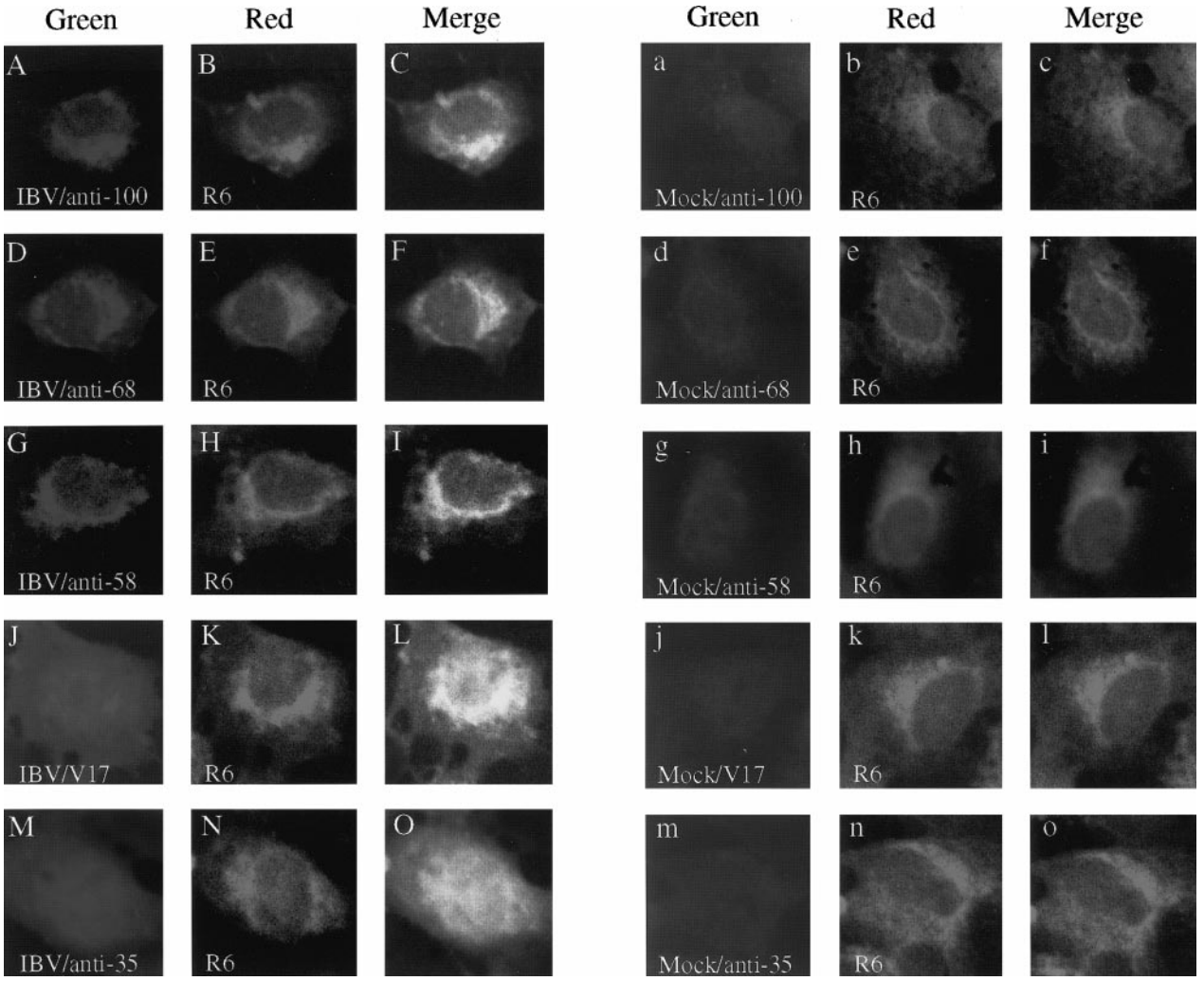


FIG. 5. Subcellular localization of the 100-, 68-, 58-, 39-, and 35-kDa proteins in transfected Cos-7 cells. Cos-7 cells were transfected with constructs encoding the 100 (A)-, 68 (D)-, 58 (G)-, 39 (J)-, and 35-kDa (M) proteins, respectively, and detected using polyclonal antibodies against the individual proteins. The proteins were labeled with the FITC-conjugated secondary antibodies. Panels B, E, H, K, and N refer to cells stained with R6, a dye for the ER. The green images represent FITC-derived green fluorescence, and red images represent rhodamine and Texas red-derived red fluorescence. Colocalization of viral proteins with the organelle markers is represented by the yellow region within each cell in the merged images (C, F, I, L, and O). Panels a–o show Cos-7 cells transfected with the empty vector pKT0 and stained with antisera or R6 as indicated. The fluorescence was viewed using a confocal scanning Zeiss microscope.

products detected in IBV-infected cells (Fig. 4, lanes 9–11).

As mentioned earlier, the apparent molecular mass and processing pattern of the 132-kDa protein suggested that it may be derived from the C-terminal region of the 1a/1b polyprotein covering the 58-, 39-, and 35-kDa proteins. To further confirm this possibility, plasmid pIBV1b4, which covers nucleotides 16932–20490 and therefore encodes the 132-kDa product (Liu *et al.,* 1998), was expressed in Cos-7 cells. As expected, immunoprecipitation of cell lysates prepared from cells transfected with pIBV1b4 with anti-58 resulted in the detection of the full-length 132-kDa protein, which comigrated on SDS–PAGE with the 132-kDa intermediate cleavage detected from cells transfected with p3C-CITE-IBV20 (Fig. 4, lanes 12 and 13).

### Subcellular localization of the cleavage products

To gain clues of the functions of the five cleavage products in the viral replication cycle, indirect immunofluorescence analysis of cells expressing individual cleavage products was carried out and representative confocal microscopy images are present in Fig. 5. Upon overexpression in Cos-7 cells, the 100-, 68-, and 58-kDa proteins exhibit similar reticular staining patterns (Figs. 5A, 5D, and 5G). These fluorescent profiles overlap with the staining patterns of R6 (Rhodamine B hexylester chloride, Molecular Probes), a short-chain carbocyanine dye known to stain membranes of the ER (Arregui *et al.,* 1998; Barsony *et al.,* 1997; Lim and Liu, 2001; Terasaki and Reese, 1992; Yang *et al.,* 1997) (Figs. 5A–5I). In Cos-7 cells, the staining pattern of R6 overlaps with the immu-

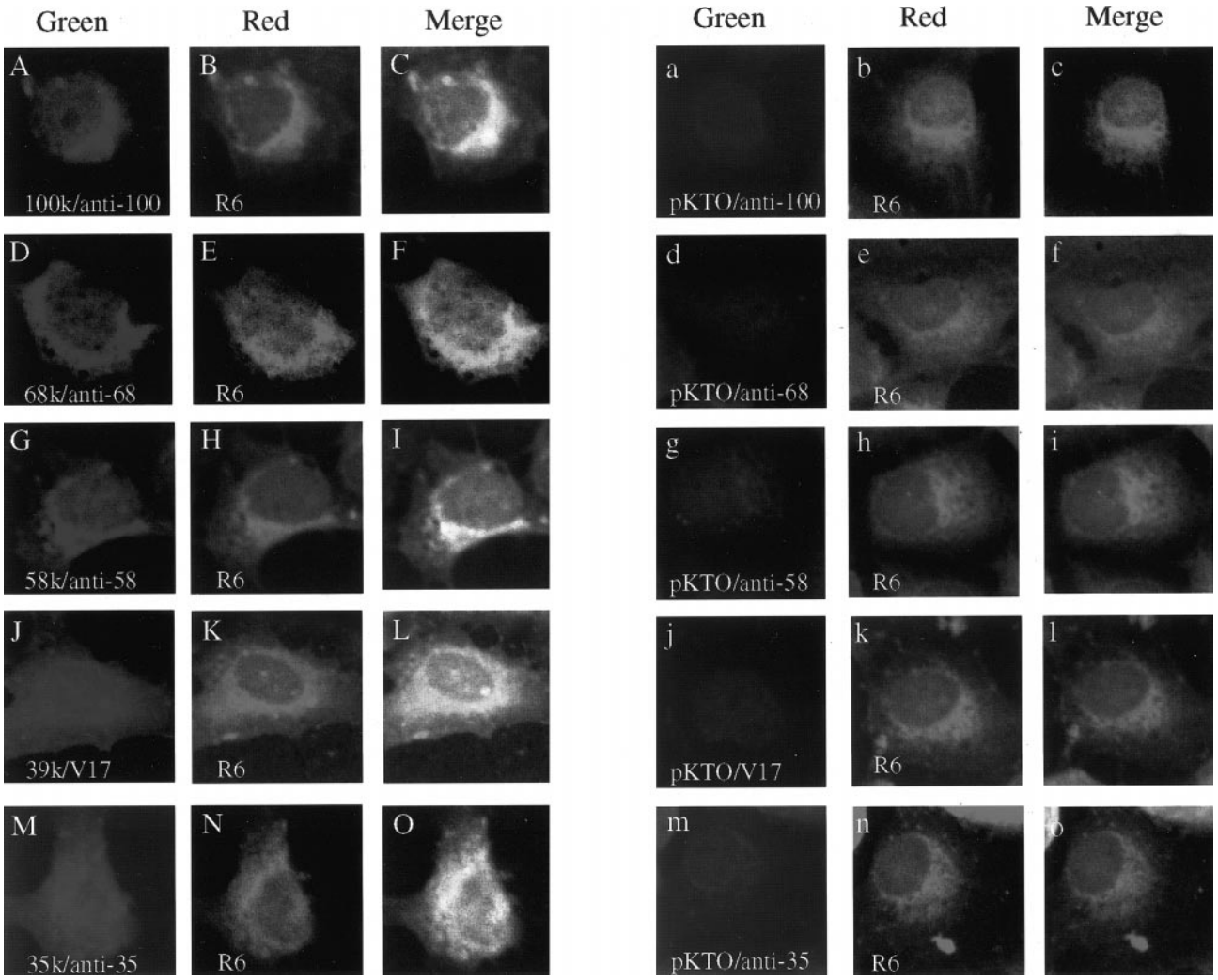


FIG. 6. Subcellular localization of the 100-, 68-, 58-, 39-, and 35-kDa proteins in IBV-infected Vero cells. Vero cells were infected with IBV at a m.o.i. of 3 PFU per cell and were detected with polyclonal antibodies against the 100 (A)-, 68 (D)-, 58 (G)-, 39 (J)-, and 35-kDa (M) proteins, respectively. Panels B, E, H, K, and N refer to cells stained with R6. The green images represent FITC-derived green fluorescence, and red images represent rhodamine and Texas red-derived red fluorescence. Colocalization of viral proteins with the organelle markers is represented by the yellow region within each cell in the merged images (C, F, I, L, and O). Panels a–o show staining of mock-infected Vero cells with antisera or R6 as indicated. The fluorescence was viewed using a confocal scanning Zeiss microscope.

nofluorescent pattern of anti-PDI (data not shown). These results suggest that the three proteins may be associated with the ER membranes. In cells expressing the 39- and 35-kDa proteins, a diffuse staining pattern was observed for each protein (Figs. 5J and 5M), which does not coalign with the staining pattern of R6 (Figs. 5J–5O). This diffuse distribution pattern of the 39- and 35-kDa proteins was unexpected, as the majority of cleavage products were shown to be membrane-associated. The same antisera were used to stain cells transfected with the empty vector pKT0 (Liu *et al.,* 1994), showing weak background staining (Figs. 5a–5o).

The subcellular localization patterns of the five proteins were then analyzed in IBV-infected cells (Fig. 6). Immunofluorescent staining of IBV-infected Vero cells with anti-100, anti-68, and anti-58, respectively, showed similar ER localization profiles (Figs. 6A–6I), and a diffuse staining pattern was observed in cells stained with antiserum V17, which reacts with both the 39- and 35-kDa proteins (Figs. 6J–6L). Similarly, a diffuse distribution pattern was observed in cells stained with anti-35 (Figs. 6M–6O). The same antisera were used to stain mock-infected cells, showing weak background staining (Figs. 6a–6o).

## DISCUSSION

In our previous reports, we showed the identification of three mature cleavage products of 100, 39, and 35 kDa, processed from the 1b region of the 1a/1b polyprotein (Liu *et al.,* 1994, 1998). However, we were unable to detect the two other cleavage products of 68 and 58 kDa.

In this study, we report the identification of the 68- and 58-kDa proteins in IBV-infected cells. In addition, two stable intermediate cleavage products of 160 and 132 kDa, respectively, were identified, which coexist with the mature cleavage products in virus-infected cells. Immunofluorescence analysis showed that the polymerase domain-containing 100-kDa protein and the helicase domain-containing 68-kDa protein as well as the 58-kDa protein may be associated with the ER and IC membranes, the viral replication and assembly sites. However, the 39- and 35-kDa proteins display diffuse distribution patterns in both IBV-infected cells and cells expressing each of the proteins.

It is intriguing that immunoprecipitation and Western blot of IBV-infected cells harvested at 8 h postinfection failed to detect the 68-kDa protein. The protein was detected by Western blot in IBV-infected cells harvested at 24 and 32 h postinfection. As the equivalent human coronavirus 71-kDa protein was shown to be an RNA helicase (Heusipp *et al.,* 1997a; Seybert *et al.,* 2000a,b), this protein is likely the IBV helicase. It is expected that such a functional product directly involved in viral RNA replication would be expressed at early stages of the viral replication cycle. In fact, the equivalent 71-kDa protein of human coronavirus was first seen in virus-infected cells at 5 h postinfection (Heusipp *et al.,* 1997a). The reason for the failure to detect the 68-kDa protein in IBV-infected cells at earlier time point is uncertain, but it might reflect the folding property, as discussed later, of the protein. The dramatic increase in the detection of the 68-kDa protein at 24 and 32 h postinfection may partially be due to the secondary infection of cells that remain uninfected during the primary infection. As significantly more cells (over 95% of cells) were infected at 24–32 h postinfection, it is understandable that more protein would be detected. A slight, but gradual increase of the accumulation of the human coronavirus 71-kDa protein over a time course of 15 h was also observed (Heusipp *et al.,* 1997a). Alternatively, the increase in the detection of the 68-kDa protein at 24–32 h postinfection may reflect the genuine accumulation pattern of the protein in virus-infected cells at late stages of the viral replication cycle. If this were the case, it may indicate that the protein might also be involved in processes other than viral RNA replication.

The identification of two stable intermediate cleavage products of 160 and 132 kDa coexisting with the mature cleavage products raised two interesting questions. First, the two products may have certain functions during the viral replication cycle. The 160-kDa product is particularly interesting in this aspect, considering the fact that it contains both the polymerase and helicase domains and the 68-kDa helicase protein is undetectable at early stages of infection. It is plausible that the 160-kDa protein might have both polymerase and helicase functions in the replication of viral RNA at early stages of the infection. In fact, some smaller positive-stranded RNA viruses encode single proteins containing both the polymerase and helicase domains (Buck, 1996). The second interesting question is why only these two intermediate cleavage products were detectable in IBV-infected cells. As shown in Fig. 4 as well as in our previous report (Liu *et al.,* 1998), other intermediate cleavage products were also observed when this region was expressed in intact cells. One obvious distinct feature of the cleavage site between these two products is that it is a Q–G dipeptide bond, while all the other cleavage sites in this region of the polyprotein are Q–S dipeptide bonds (Fig. 1). However, no experimental data indicate that cleavage at the Q–G site is more efficient than at the Q–S sites.

The 68-kDa protein migrated on SDS–PAGE as a multiprotein species, heterogeneous smear, probably due to the formation of protein aggregates, and deletion analysis showed that a stretch of 30 amino acid residues in the C-terminal region was responsible for the aberrant migration property of the protein (data not shown). It suggests that the 68-kDa protein may misfold when expressed in intact cells in the absence of other viral components. In recent years, it was found that the proper folding of certain proteins requires the assistance of molecular chaperones (Ellis and van der Vies, 1991; Gething and Sambrook, 1992). As the 68-kDa protein may be a component of the viral RNA replication complex, the protein is expected to interact with viral RNA and other viral proteins. Those viral RNA/proteins may act as a chaperone for the correct folding of the 68-kDa protein in IBV-infected cells. It would be of interest to define if the region of the 30 amino acid residues that were shown to be responsible for the aberrant migration of the 68-kDa protein on SDS–PAGE contain either RNA binding or protein interacting domains. However, no such domains were found in this or the neighboring regions by computer analysis using relevant programs.

The 58-kDa protein was recently shown to be able to induce programmed cell death when expressed alone in intact cells (Liu *et al.,* 2001). This is the first IBV product that was demonstrated to be a proapoptotic protein. In our previous report, we were unable to identify the 58-kDa protein in IBV-infected cells due to the cross-reactivity of the antiserum used with a cellular protein (Liu *et al.,* 1998). A newly raised antiserum was used in this study, leading to the successful identification of the protein in virus-infected cells. Understanding of the expression, processing, and subcellular distribution pattern of the 58-kDa protein would help us to further characterize the proapoptotic property of the protein and to study the functions of the protein in the pathogenesis of IBV-induced infection in chicken, the natural host of IBV.

Currently, no functions have been assigned to the 39- and 35-kDa proteins. A counterpart of the IBV 39-kDa protein, the 41-kDa protein of human coronavirus, was shown to exhibit a punctate, perinuclear distribution pat-

tern in virus-infected cells (Heusipp *et al.,* 1997b). Interestingly, the 39- and 35-kDa proteins display a diffuse distribution pattern in both IBV-infected cells and in cells overexpressing the proteins. As the majority of the cleavage products from the 1a and 1a/1b polyproteins were shown to be associated with cellular membranes at or near the viral replication and assembly sites, the diffuse distribution pattern may exclude the direct involvement of the two proteins in the formation of viral replication complexes.

## MATERIALS AND METHODS

### Virus and cells

The egg-adapted Beaudette strain of IBV (ATCC VR-22) was obtained from the American Type Culture Collection (ATCC) and was adapted to Vero cells as described by Alonso-Caplen *et al.* (1984). Briefly, the virus was passaged three times in 11-day-old chicken embryos and then adapted to Vero cells (ATCC CCL-81) by a series of passages at 24–48 h intervals. The cytopathic effects, including syncytium formation and rounding up of cells, were initially observed after three passages in Vero cells. Virus stocks were prepared after the 36th passage by infecting monolayers of Vero cells at a m.o.i. of approximately 0.1 PFU/cell. The virus was harvested at 24 h postinfection and the titer of the virus preparation was determined by plaque assay on Vero cells.

Vero cells were grown at 37°C in 5% $CO_2$ and maintained in Glasgow's modified minimal essential medium (GMEM) supplemented with 10% newborn calf serum.

### Labeling of IBV-infected cells with [$^{35}$S]methionine

Confluent monolayers of Vero cells were infected with IBV at a m.o.i. of approximately 3 PFU/cell. Prior to being labeled, the cells were incubated in methionine-free medium for 30 min. After 4 h of labeling with 25 $\mu$Ci of [$^{35}$S]methionine, the cells were scraped off the dishes in phosphate-buffered saline (PBS), recovered by centrifugation, and stored at −80°C.

### Transient expression of IBV sequences in Vero cells using a vaccinia-T7 expression system

Open reading frames placed under control of the T7 promoter were expressed transiently in eukaryotic cells as described previously (Liu *et al.,* 1994). Briefly, semiconfluent monolayers of Vero cells were infected with 10 PFU/cell of a recombinant vaccinia virus (vTF7-3) which expresses the bacteriophage T7 RNA polymerase and then transfected with appropriate plasmid DNA using the DOTAP transfection reagent according to the instructions of the manufacturer (Roche). After incubation of the cells at 37°C for 4 h, 25 $\mu$Ci/ml of [$^{35}$S]methionine was added directly to the medium. The radiolabeled cells were harvested at 18 h posttransfection.

### Polymerase chain reaction (PCR)

Appropriate primers and template DNAs were used in amplification reactions with *Pfu* DNA polymerase (Stratagene) under standard buffer conditions with 2 mM $MgCl_2$. The PCR conditions were 30 cycles of 95°C for 45 s, *X*°C for 45 s, and 72°C for *X* min. The annealing temperature (*X*°C) and the extension time (*X* min) were adjusted according to the melting temperature of the primers used and the length of the PCR fragments synthesized.

### Radioimmunoprecipitation

Plasmid DNA-transfected Vero cells were lysed with RIPA buffer (50 mM Tris–HCl, pH 7.5, 150 mM NaCl, 1% sodium deoxycholate, 0.1% SDS, 1% NP-40) and precleared by centrifugation at 12,000 rpm for 5 min at 4°C in a microfuge. Immunoprecipitation was carried out as described previously (Liu *et al.,* 1994).

### SDS–polyacrylamide gel electrophoresis

SDS–polyacrylamide gel electrophoresis (SDS–PAGE) of virus polypeptides was carried out using 12.5% polyacrylamide gels (Laemmli, 1970). Labeled polypeptides were detected by autoradiography or fluorography of dried gels.

### Indirect immunofluorescence microscopy and confocal microscopy

Cells were grown on four-well chamber slides (Iwaki) and infected with IBV or transfected with appropriate plasmid DNAs. After washing with PBS, the cells were fixed with 4% paraformaldehyde (in PBS) for 15 min at room temperature and permeabilized with 0.2% Triton X-100 (in PBS), followed by incubation with specific antiserum at room temperature for 2 h. Antibodies were diluted in fluorescence dilution buffer (PBS with 5% normal goat serum). The cells were then washed with PBS and incubated with anti-rabbit IgG conjugated to fluorescein isothiocynate (FITC) (Sigma) in the fluorescence dilution buffer at 4°C for 1 h before mounting.

Confocal microscopy was performed on a Zeiss Axioplan microscope connected to a Bio-Rad MRC 1024 laser scanner equipped with an argon laser with appropriate filters. Fluorescent images were superimposed to allow fine comparison and colocalization of green (FITC) and red (TRITC) signals in a single pixel produces yellow, while separated signals are green or red.

### Construction of plasmids

Plasmid pIBV1b4, which contains nucleotides 16932–20490, was previously described (Liu *et al.,* 1998).

Plasmid pIBV1b3 contains nucleotides 15132–16931 and codes for the 68-kDa protein, pIBV1b6 contains nucleotides 16930–18495 and codes for the 58-kDa protein,

pIBV1b9 contains nucleotides 18496–19508 and codes for the 39-kDa protein, and pIBV1b10 contains nucleotides 19509–20506 and codes for the 35-kDa protein. These constructs were made by cloning an *Nco*I- and *Bam*HI-digested PCR fragment into *Nco*I- and *Bam*HI-digested pKT0 (Liu *et al.,* 1994). The sequences of the two primers used to construct pIBV1b3 were 5′-CGACTTCCATGGCTTGTGGCGTT′-3 and 5′-CCAAAGGATCCTATTGCAGACTTG-3′. The sequences of the two primers used to construct pIBV1b6 were 5′-ACAAGTCCCATGGGTACAGGTT-3′ and 5′-TATTGGATCCTACGGAGAGCTG-3′. The sequences of the two primers used to construct pIBV1b9 were 5′-GTTTTTCAGCTCCCATGGCTATCGACAAT-3′ and 5′-AACCACACGTCGGATCCTATTGAAGCTGTG-3′. The sequence of the two primers used to construct pIBV1b10 was 5′-CCACAGCTTCCCATGGCATGGACGTG-3′.

Plasmid pIBVpol, which contains nucleotides 12451–15131 and codes for the 100-kDa protein with a 37-amino-acid truncation at the N-terminus, was constructed by cloning a *Bam*HI- and *Xho*I-digested PCR fragment into *Bam*HI- and *Xho*I-digested pET22b(+) (Novagen). The sequences of the primers used were 5′-GTAATAAGGATCCAGCTGGTATG-3′ and 5′-AAGGCCTCGAGTTGTAAAGTCGTAGGAGC-3′.

The two dicistronic constructs, p3C-CITE-IBV20 and p3C-CITE-IBV8, were constructed as follows. The IRES sequence was obtained by digestion of pCITE-1 (Novagen) with *Eco*RI, end-repair with Klenow, and redigestion with *Nco*I. This 592-bp fragment was then cloned into *Pvu*II- and *Nco*I-digested pKT0, giving rise to pKT-CITE. The IBV sequence that codes for the 3C-like proteinase was obtained by digestion of pIBV3C (Liu *et al.,* 1997) with *Bgl*II and *Bam*HI and was cloned into *Bgl*II-digested pKT-CITE, giving rise to p3C-CITE. Digestion of p3C-CITE with *Nco*I produced a 1510-bp fragment containing both the IBV 3C-like proteinase and the IRES sequences. This fragment was then cloned into *Nco*I-digested pIBV1b8 and pIBV20, respectively, creating the two dicistronic constructs. Plasmids pIBV1b8 and pIBV20, which cover the IBV sequences from nucleotides 15132 to 18495 and 15132 to 20506, respectively, were constructed by cloning *Nco*I- and *Bam*HI-digested PCR fragments covering the relevant regions into *Nco*I- and *Bam*HI-digested pKT0.

## ACKNOWLEDGMENT

This work was supported by the National Science and Technology Board of Singapore.

## REFERENCES

Alonso-Caplen, F. V., Matsuoka, Y., Wilcox, G. E., and Compans, R. W. (1984). Replication and morphogenesis of avian coronavirus in Vero cells and their inhibition by monensin. *Virus Res.* **1,** 153–167.

Arregui, C. O., Balsamo, J., and Lilien, J. (1998). Impaired integrin-mediated adhesion and signaling in fibroblasts expressing a dominant-negative mutant PTP1B. *J. Cell Biol.* **143,** 861–873.

Barsony, J., Renyi, I., and McKoy, W. (1997). Subcellular distribution of normal and mutant vitamin D receptors in living cells. *J. Biol. Chem.* **272,** 5774–5782.

Bost, A. G., Carnahan, R. H., Lu, X. T., and Denison, M. R. (2000). Four proteins processed from the replicase gene polyprotein of mouse hepatitis virus colocalize in the cell periphery and adjacent to sites of virion assembly. *J. Virol.* **74,** 3379–3387.

Boursnell, M. E. G., Brown, T. D. K., Foulds, I. J., Green, P. F., Tomely, F. M., and Binns, M. M. (1987). Completion of the sequence of the genome of the coronavirus avian infectious bronchitis virus. *J. Gen. Virol.* **68,** 57–77.

Buck, K. W. (1996). Comparison of the replication of positive-stranded RNA viruses of plants and animals. *Adv. Virus Res.* **47,** 159–251.

Denison, M. R., Spaan, W. J., van der Meer, M. Y., Gibson, C. A., Sims, A. C., Prentice, E., and Lu, X. T. (1999). The putative helicase of the coronavirus mouse hepatitis virus is processed from the replicase gene polyprotein and localizes in complexes that are active in viral RNA synthesis. *J. Virol.* **73,** 6862–6871.

Ellis, R. J., and van der Vies, S. M. (1991). Molecular chaperones. *Annu. Rev. Biochem.* **60,** 321–347.

Fuerst, T. R., Niles, E. G., Studier, F. W., and Moss, B. (1986). Eukaryotic transient-expression system based on recombinant vaccinia virus that synthesizes bacteriophage T7 RNA polymerase. *Proc. Natl. Acad. Sci. USA* **83,** 8122–8127.

Gething, M.-J., and Sambrook, J. (1992). Protein folding in the cell. *Nature* **355,** 33–45.

Heusipp, G., Harms, U., Siddell, S. G., and Ziebuhr, J. (1997a). Identification of an ATPase activity associated with a 71-kilodalton polypeptide encoded in gene 1 of the human coronavirus 229E. *J. Virol.* **71,** 5631–5634.

Heusipp, G., Grotzinger, C., Herold, J., Siddell, S. G., and Ziebuhr, J. (1997b). Identification and subcellular localization of a 41 kDa, polyprotein 1ab processing product in human coronavirus 229E-infected cells. *J. Gen. Virol.* **78,** 2789–2794.

Laemmli, U. K. (1970). Cleavage of structural proteins during the assembly of the head of bacteriophage T4. *Nature (London)* **227,** 680–685.

Lim, K. P., and Liu, D. X. (1998). Characterization of the two overlapping papain-like proteinase domains encoded in gene 1 of the coronavirus infectious bronchitis virus and determination of the C-terminal cleavage site of an 87 kDa protein. *Virology* **245,** 303–312.

Lim, K. P., Ng, L. F. P., and Liu, D. X. (2000). Identification of a novel cleavage activity of the first papain-like proteinase domain encoded by ORF 1a of the coronavirus avian infectious bronchitis virus and characterization of the cleavage products. *J. Virol.* **74,** 1674–1685.

Lim, K. P., and Liu, D. X. (2001). The missing link in coronavirus assembly: Retention of the avian coronavirus infectious bronchitis virus envelope protein in the pre-Golgi compartments and physical interaction between the envelope and membrane proteins. *J. Biol. Chem.* **276,** 17515–17523.

Liu, C., Xu, H. Y., and Liu, D. X. (2001). Induction of caspase-dependent apoptosis in cultured cells by the avian coronavirus infectious bronchitis virus. *J. Virol.* **75,** 6402–6409.

Liu, D. X., and Brown, T. D. K. (1995). Characterisation and mutational analysis of an ORF 1a-encoding proteinase domain responsible for proteolytic processing of the infectious bronchitis virus 1a/1b polyprotein. *Virology* **209,** 420–427.

Liu, D. X., Brierley, I., Tibbles, K. W., and Brown, T. D. K. (1994). A 100-kilodalton polypeptide encoded by open reading frame (ORF) 1b of the coronavirus infectious bronchitis virus is processed by ORF 1a products. *J. Virol.* **68,** 5772–5780.

Liu, D. X., Tibbles, K. W., Cavanagh, D., Brown, T. D. K., and Brierley, I. (1995). Identification, expression, and processing of an 87-kDa polypeptide encoded by ORF 1a of the coronavirus infectious bronchitis virus. *Virology* **208,** 48–57.

Liu, D. X., Xu, H. Y., and Brown, T. D. K. (1997). Proteolytic processing of the coronavirus infectious bronchitis virus 1a polyprotein: Identification of a 10 kDa polypeptide and determination of its cleavage sites. *J. Virol.* **71,** 1814–1820.

Liu, D. X., Shen, S., Xu, H. Y., and Wang, S. F. (1998). Proteolytic mapping of the coronavirus infectious bronchitis virus 1b polyprotein: evidence for the presence of four cleavage sites of the 3C-like proteinase and identification of two novel cleavage products. *Virology* **246,** 288–297.

Ng, L. F. P., and Liu, D. X. (1998). Identification of a 24 kDa polypeptide processed from the coronavirus infectious bronchitis virus 1a polyprotein by the 3C-like proteinase and determination of its cleavage sites. *Virology* **243,** 388–395.

Ng, L. F. P., and Liu, D. X. (2000). Further characterization of the coronavirus infectious bronchitis virus 3C-like proteinase and determination of a new cleavage site. *Virology* **272,** 27–39.

Schiller, J. J., Kanjanahaluethai, A., and Baker, S. C. (1998). Processing of the coronavirus MHV-JHM polymerase polyprotein: identification of precursors and proteolytic products spanning 400 kilodaltons of ORF1a. *Virology* **242,** 288–302.

Seybert, A., Hegyi, A., Siddell, S. G., and Ziebuhr, J. (2000a). The human coronavirus 229E superfamily 1 helicase has RNA and DNA duplex-unwinding activities with 5′–3′ polarity. *RNA* **6,** 1056–1068.

Seybert, A., van Dinten, L. C., Snijder, E. J., and Ziebuhr, J. (2000b). Biochemical characterization of the equine arteritis virus helicase suggests a close functional relationship between arterivirus and coronavirus helicases. *J. Virol.* **74,** 9586–9593.

Shi, S. T., Schiller, J. J., Kanjanahaluethai, A., Baker, S. C., Oh, J.-W., and Lai, M. M. C. (1999). Colocalization and membrane association of murine hepatitis virus gene 1 products and de novo-synthesized viral RNA in infected cells. *J. Virol.* **73,** 5957–5969.

Sims, A. C., Ostermann, J., and Denison, M. R. (2000). Mouse hepatitis virus replicase proteins associate with two distinct populations of intracellular membranes. *J. Virol.* **74,** 5647–5654.

Terasaki, M., and Reese, T. S. (1992). Characterization of endoplasmic reticulum by colocalization of B-p and dicarbocyanine dyes. *J. Cell Sci.* **101,** 315–322.

van der Meer, Y., Snijder, E. J., Dobbe, J. C., Schleich, S., Denison, M. R., Spaan, W. J. M., and Locker, J. K. (1999). Localization of mouse hepatitis virus nonstructural proteins and RNA synthesis indicates a role for late endosomes in viral replication. *J. Virol.* **73,** 7641–7657.

Yang, L., Guan, T., and Gerace, L. (1997). Integral membrane proteins of the nuclear envelope are dispersed throughout the endoplasmic reticulum during mitosis. *J. Cell Biol.* **137,** 1199–1210.

Ziebuhr, J., and Siddell, S. G. (1999). Processing of the human coronavirus 229E replicase polyproteins by the virus-encoded 3C-like proteinase: Identification of proteolytic products and cleavage sites common to pp1a and pp1ab. *J. Virol.* **73,** 177–185.

Ziebuhr, J., Snijder, E. J., and Gorbalenya, A. E. (2000). Virus encoded proteinases and proteolytic processing in the Nidovirales. *J. Gen. Virol.* **81,** 853–879.